Automatica 54 (2015) 72–79

Contents lists available at ScienceDirect

Automatica

journal homepage: www.elsevier.com/locate/automatica

Brief paper

Distributed state estimation for linear multi-agent systems with time-varying measurement topology☆

Daniel Viegas [a], Pedro Batista [a], Paulo Oliveira [a,b], Carlos Silvestre [a,c], C.L. Philip Chen [d]

[a] Institute for Systems and Robotics, Instituto Superior Técnico, Av. Rovisco Pais, 1049-001 Lisboa, Portugal

[b] Department of Mechanical Engineering, Instituto Superior Técnico, Universidade de Lisboa, Lisboa, Portugal

[c] Department of Electrical and Computer Engineering, Faculty of Science and Technology, University of Macau, Taipa, Macau

[d] Department of Computer and Information Science, Faculty of Science and Technology, University of Macau, Taipa, Macau

ARTICLE INFO

Article history:
Received 12 June 2013
Received in revised form
14 November 2014
Accepted 16 January 2015

Keywords:
Multi-agent systems
Decentralization
Navigation and cooperative navigation techniques
Autonomous systems
Underwater vehicles

ABSTRACT

This paper addresses the problem of distributed state estimation in formations of vehicles with time-varying measurement topology. One or more vehicles have access to measurements of their own state, while the rest must rely on measurements relative to other vehicles in the vicinity and limited communication to estimate their own state, and it is assumed that the vehicles may gain or lose access to some measurements over time. The proposed solution consists in the implementation of a local state observer on-board each vehicle, and the effects of changes in the measurement topology on the estimation error dynamics are studied resorting to switched systems theory. Sufficient conditions for exponential stability of the global estimation error dynamics are presented for two different switching laws. The results are applied to the practical case of a formation of Autonomous Underwater Vehicles (AUVs), and simulation results are presented that validate the proposed solution.

1. Introduction

Motivated by the wealth of potential applications for formations composed of multiple agents working cooperatively, see e.g. Bender (1991), Curtin, Bellingham, and Webb (1993), and Giulietti, Pollini, and Innocenti (2000), the subjects of estimation and control in formations of vehicles have been researched extensively in the past few years. The various solutions proposed by the research community can be divided into two very broad categories: centralized and decentralized solutions. Centralized solutions consider the formation as a whole and rely on a central processing node to perform most of the computations, allowing the use of classical, single-vehicle solutions to tackle the multi-agent problem. However, implementation is almost guaranteed to be cumbersome, as heavy computational and communication loads are to be expected due to the necessity of conveying all the information in the formation to a central processing node, which must then relay the results of its computations back to the vehicles. To avoid those pitfalls, the aim of decentralized solutions is to break down the problem in several parts, leaving each agent in the formation with the responsibility of performing a subset of the computations, relying on limited information and communication with other vehicles in the formation. On the subject of decentralized and distributed state estimation, interesting approaches can be found in works such as Barooah (2007), Sousa, Oliveira, and Gaspar (2009), and Yuan and Tanner (2010). The closely related area of distributed control has also seen a wealth of relevant solutions, such as those in Chen, Wen, Liu, and Wang (2014), Fax (2002), and Tanner and Christodoulakis (2007), and recent work on the subject of quadratic invariance has offered optimal solutions for certain classes of measurement topologies, see e.g. Lessard and Lall (2011) and Rokowitz (2008).

The problem addressed in this paper is the design of a distributed state observer for a formation of autonomous vehicles with time-varying measurement topology. One or more vehicles have access to measurements of their own state, while the rest must rely on measurements relative to other vehicles in the vicinity and limited communication with those agents in order to estimate their state. Between switches in the measurement topology, the vehicles only communicate state estimates to use as

☆ The material in this paper was partially presented at the 2013 American Control Conference, June 17–19, 2013, Washington, DC, USA. This paper was recommended for publication in revised form by Associate Editor Abdelhamid Tayebi under the direction of Editor Toshiharu Sugie.

E-mail addresses: dviegas@isr.ist.utl.pt (D. Viegas), pbatista@isr.ist.utl.pt (P. Batista), pjcro@isr.ist.utl.pt (P. Oliveira), csilvestre@umac.mo (C. Silvestre), philipchen@umac.mo (C.L.P. Chen).

http://dx.doi.org/10.1016/j.automatica.2015.01.036
0005-1098/

comparison terms for the relative measurements. When there are changes in the measurement topology, the vehicles also need to exchange tables of edges and control vectors with other agents in the vicinity to recover the new measurement graph.

The problem is formulated as a state observer design problem with a sparsity constraint on the output injection gains to reflect the limited amount of information available to each agent. In Viegas, Batista, Oliveira, and Silvestre (2012), the problem was addressed for the fixed topology case, that is, when the measurements available to each vehicle remain the same over time. However, as sensing and communication in formations of vehicles can be unreliable in most practical cases, it is assumed that the measurements available to the agents can change over time, resulting in a time-varying measurement topology. To address this issue, a strategy is outlined for the vehicles to cope with the changes in the measurements, and a switched systems approach is employed to study the stability of the distributed state observer. The error dynamics are formulated as a switched linear system, and sufficient conditions for their exponential stability are derived for two different switching laws. These stability results can be used by mission planners for multi-agent systems as they establish requirements for the behavior of the formation and the sensing and communication equipment of each vehicle that guarantee position and velocity estimates with stable error dynamics over the course of the mission. The behavior of this solution is then assessed in simulation for a formation of Autonomous Underwater Vehicles (AUVs). Preliminary results on this subject can be found in Viegas, Batista, Oliveira, and Silvestre (2013). This paper extends this work with more complete theoretical results, and a more thorough treatment of the transition periods between stable configurations.

The rest of the paper is organized as follows. Section 2 describes the problem at hand and introduces the dynamics of the vehicles and their respective local observers, while Section 3 details the framework necessary to describe the formation-wide dynamics. Section 4 outlines the strategy followed by the vehicles to cope with changes in the measurement topology, and in Section 5 the stability of the error dynamics is analyzed. Section 6 presents simulation results for a formation of AUVs and, finally, Section 7 summarizes the main conclusions of the paper.

1.1. Notation

Throughout the paper the symbol $\mathbf{0}$ denotes a matrix (or vector) of zeros and $\mathbf{I}$ an identity matrix, both of appropriate dimensions. Whenever relevant, the dimensions of an $n \times n$ identity matrix are indicated as $\mathbf{I}_n$. The Kronecker product of two matrices $\mathbf{A}$ and $\mathbf{B}$ is denoted by $\mathbf{A} \otimes \mathbf{B}$. For $x \in \mathbb{R}$, $\lfloor x \rfloor$ represents the largest integer not larger than x.

2. Problem statement

Consider a formation composed of N autonomous vehicles, in which each vehicle is indexed by a distinct positive integer $i \in \{1, 2, \ldots, N\}$, and has sensors mounted on-board which give access to either:

- measurements based on its own state, denoted as "absolute" measurements for convenience; or
- measurements based on its state relative to N_i other vehicles in the vicinity. Furthermore, it is assumed that those vehicles send updated state estimates to vehicle i through communication.

The problem considered in this paper is the design of a distributed state observer that allows each vehicle to estimate its state based primarily on the aforementioned measurements, as well as limited communication between vehicles. The solution proposed here consists in the implementation of a local state observer on-board each vehicle. To achieve a decentralized structure, those local observers must be designed such that, during operation, each vehicle only requires locally available measurements and limited communication with other vehicles in its vicinity to estimate its state. Doing this allows to greatly reduce the communication and computational load in the formation in comparison with a standard centralized implementation, in which all measurements would need to be communicated to a central processing node, which would then perform all the computations and then broadcast the state estimates to the whole formation. This is specially relevant in cases where communication between agents is challenging, such as in underwater applications, or when strict limits on the payload condition the processing, sensing, and communication equipment that can be mounted on-board each vehicle, such as with airborne vehicles.

This section details the dynamics of the vehicles and their respective local state observers, leaving the analysis of the formation-wide dynamics to subsequent sections.

2.1. Local state observer design

For a vehicle i which has access to absolute measurements, its dynamics are described by the Linear Time-Invariant (LTI) system

$$\begin{cases} \dot{\mathbf{x}}_i(t) = \mathbf{A}_L \mathbf{x}_i(t) + \mathbf{B}_L \mathbf{u}_i(t) \\ \mathbf{y}_i(t) = \mathbf{C}_L \mathbf{x}_i(t), \end{cases} \tag{1}$$

where $\mathbf{x}_i(t) \in \mathbb{R}^{n_L}$ is the state of vehicle i, to be estimated, $\mathbf{u}_i(t) \in \mathbb{R}^{m_L}$ is the input of the system, and $\mathbf{y}_i(t) \in \mathbb{R}^{o_L}$ is the output. $\mathbf{A}_L$, $\mathbf{B}_L$, and $\mathbf{C}_L$ are given constant matrices of appropriate dimensions. For this case, it is straightforward to design a Luenberger observer with globally exponentially stable error dynamics, see e.g. Astrom and Murray (2008). On the other hand, if vehicle i has access to relative measurements to N_i other vehicles in the formation, its dynamics follow

$$\begin{cases} \dot{\mathbf{x}}_i(t) = \mathbf{A}_L \mathbf{x}_i(t) + \mathbf{B}_L \mathbf{u}_i(t) \\ \mathbf{y}_i(t) = \mathbf{C}_i \Delta\mathbf{x}_i(t), \end{cases} \tag{2}$$

in which $\mathbf{y}_i(t) \in \mathbb{R}^{o_L \times N_i}$, $\mathbf{C}_i = \mathbf{I}_{N_i} \otimes \mathbf{C}_L$, and

$$\Delta\mathbf{x}_i(t) := \begin{bmatrix} \mathbf{x}_i(t) - \mathbf{x}_{\theta_{i,1}}(t) \\ \mathbf{x}_i(t) - \mathbf{x}_{\theta_{i,2}}(t) \\ \vdots \\ \mathbf{x}_i(t) - \mathbf{x}_{\theta_{i,N_i}}(t) \end{bmatrix} \in \mathbb{R}^{n_L N_i}, \quad \theta_{i,j} \in \Theta_i,$$

where

$$\Theta_i := \left\{ \theta_{i,1}, \theta_{i,2}, \ldots, \theta_{i,N_i} | \theta_{i,j} \in \{1, \ldots, N\} \right\}$$

is the set of other vehicles' indexes corresponding to the relative measurements available to vehicle i. For this case, the following local observer structure for the system (2) can be implemented:

$$\begin{cases} \dot{\hat{\mathbf{x}}}_i(t) = \mathbf{A}_L \hat{\mathbf{x}}_i(t) + \mathbf{B}_L \mathbf{u}_i(t) + \mathbf{L}_i(\mathbf{y}_i(t) - \hat{\mathbf{y}}_i(t)) \\ \hat{\mathbf{y}}_i(t) = \mathbf{C}_i \Delta\hat{\mathbf{x}}_i(t), \end{cases} \tag{3}$$

where $\mathbf{L}_i \in \mathbb{R}^{n_L \times o_L N_i}$ is a constant matrix of observer gains, to be computed, and $\Delta\hat{\mathbf{x}}_i(t)$ is an estimate of $\Delta\mathbf{x}_i(t)$, computed using the received state estimates:

$$\Delta\hat{\mathbf{x}}_i(t) := \begin{bmatrix} \hat{\mathbf{x}}_i(t) - \hat{\mathbf{x}}_{\theta_{i,1}}(t) \\ \hat{\mathbf{x}}_i(t) - \hat{\mathbf{x}}_{\theta_{i,2}}(t) \\ \vdots \\ \hat{\mathbf{x}}_i(t) - \hat{\mathbf{x}}_{\theta_{i,N_i}}(t) \end{bmatrix} \in \mathbb{R}^{n_L N_i}, \quad \theta_{i,j} \in \Theta_i.$$

3. Estimation error dynamics

The structure of the formation can be described using two graphs: a directed measurement graph $\mathcal{G}_M$ and a communication

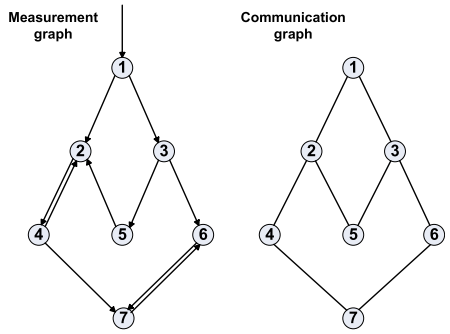

Fig. 1. Example of a measurement graph for a formation of 7 vehicles and associated communication graph which satisfies Assumption 1.

graph $\mathcal{G}_C$ (see Fig. 1 for an example with a formation of 7 vehicles). For this work, it is assumed that the communication graph is undirected, that is, all communication links are two-way. While one-way communication is relevant in some applications, it falls outside the scope of this paper as the use of directed communication graphs may significantly increase the complexity of the distributed problems addressed in Section 4 (see e.g. Barooah, 2007). In the measurement graph $\mathcal{G}_M$ each vertex represents a distinct vehicle, and an edge (a, b) means that vehicle b has access to a measurement relative to vehicle a. To represent the absolute measurements available to some of the vehicles, define a special set of edges of the form $(0, i)$, connected to only one vertex, which represents the absolute state measurement available to vehicle i.

In a similar fashion, in the communication graph $\mathcal{G}_C$ each vertex represents a distinct vehicle, and an edge (a, b) means that vehicles a and b can exchange data through some communication channel. Note that, for the vehicles to be able to implement the local state observers defined in (3), each relative measurement must be accompanied by the corresponding state estimate, received through communication. Thus, for each edge in the measurement graph $\mathcal{G}_M$ the corresponding edge must exist in the communication graph $\mathcal{G}_C$, and the following assumption is needed for the implementation of the proposed distributed state observer:

Assumption 1. If the measurement graph $\mathcal{G}_M$ contains the edge (a, b) (excluding the special edges of the form $(0, i)$), then the communication graph $\mathcal{G}_C$ also contains the edge (a, b).

The global dynamics of the formation can be represented by the LTI system

$$\begin{cases} \dot{\mathbf{x}}(t) = \mathbf{A}_g \mathbf{x}(t) + \mathbf{B}_g \mathbf{u}(t) \\ \mathbf{y}(t) = \mathbf{C}_g \mathbf{x}(t), \end{cases} \tag{4}$$

where $\mathbf{x}(t) := \begin{bmatrix} \mathbf{x}_1^T(t) & \cdots & \mathbf{x}_N^T(t) \end{bmatrix}^T \in \mathbb{R}^{n_L N}$ is the concatenation of the states of each vehicle in the formation, $\mathbf{y}(t) := \begin{bmatrix} \mathbf{y}_1^T(t) & \cdots & \mathbf{y}_N^T(t) \end{bmatrix}^T \in \mathbb{R}^{o_L M}$ is the concatenation of the measurements available to each vehicle, M being the total number of measurements in the whole formation, and $\mathbf{u}(t) := \begin{bmatrix} \mathbf{u}_1^T(t) & \cdots & \mathbf{u}_N^T(t) \end{bmatrix}^T \in \mathbb{R}^{m_L N}$ is the concatenation of the input vectors associated with each vehicle. The matrices $\mathbf{A}_g$, $\mathbf{B}_g$, and $\mathbf{C}_g$ are built from the dynamics of the individual agents, following $\mathbf{A}_g = \mathbf{I}_N \otimes \mathbf{A}_L$, $\mathbf{B}_g = \mathbf{I}_N \otimes \mathbf{B}_L$, and $\mathbf{C}_g = \mathbf{S}_{\mathcal{G}_M}^T \otimes \mathbf{C}_L$, where $\mathbf{S}_{\mathcal{G}_M}$ is the incidence matrix of the measurement graph $\mathcal{G}_M$ of the formation. The local state observers can also be grouped in a similar way, yielding

$$\begin{cases} \dot{\hat{\mathbf{x}}}(t) := \mathbf{A}_g \hat{\mathbf{x}}(t) + \mathbf{B}_g \mathbf{u}(t) + \mathbf{L}(\mathbf{y}(t) - \hat{\mathbf{y}}(t)) \\ \hat{\mathbf{y}}(t) := \mathbf{C}_g \hat{\mathbf{x}}(t), \end{cases} \tag{5}$$

where $\hat{\mathbf{x}}(t) := \begin{bmatrix} \hat{\mathbf{x}}_1^T(t) & \hat{\mathbf{x}}_2^T(t) & \cdots & \hat{\mathbf{x}}_N^T(t) \end{bmatrix}^T \in \mathbb{R}^{n_L N}$ is the concatenation of the state estimates of each vehicle in the formation, and $\mathbf{L} \in \mathbb{R}^{n_L N \times o_L M}$ is the matrix of observer gains. To account for the fact that each local observer only has access to some measurements, $\mathbf{L}$ must follow a given structural constraint. More specifically, define an augmented incidence matrix

$$\mathbf{S}'_{\mathcal{G}_M} = \mathbf{S}_{\mathcal{G}_M} \otimes \mathbf{1}_{n_L, o_L},$$

where $\mathbf{1}_{n,m}$ is a $n \times m$ matrix whose entries are all equal to 1. Then, the individual entries of $\mathbf{L}$ follow

$$\begin{cases} [\mathbf{S}'_{\mathcal{G}_M}]_{jk} = 1 \Rightarrow \mathbf{L}_{jk} \quad \text{can be set to an arbitrary value} \\ [\mathbf{S}'_{\mathcal{G}_M}]_{jk} \neq 1 \Rightarrow \mathbf{L}_{jk} = 0. \end{cases} \tag{6}$$

3.1. Computation of stable observer gains

The global error of the distributed state observer (5), $\tilde{\mathbf{x}}(t) \in \mathbb{R}^{n_L N}$, is defined as

$$\tilde{\mathbf{x}}(t) := \mathbf{x}(t) - \hat{\mathbf{x}}(t).$$

Taking its time derivative and using (4) and (5) yields

$$\dot{\tilde{\mathbf{x}}}(t) = (\mathbf{A}_g - \mathbf{L}\mathbf{C}_g)\tilde{\mathbf{x}}(t). \tag{7}$$

In this case, the computation of gains differs from standard observer design problems because the sparsity constraint in (6) must be satisfied. The problem of finding such observer gains was addressed in previous work by the authors in Viegas et al. (2012), which introduced two methods to compute gains for the distributed state observer:

- **Method 1:** If the measurement graph $\mathcal{G}_M$ associated with the formation is acyclic, the gains can be computed independently from the measurement topology and with a low computational burden, but without performance guarantees, see Viegas et al. (2012, Theorem 1);
- **Method 2:** an iterative algorithm (see Viegas et al., 2012, Table 1) to minimize the H_2 norm of the total estimation error in the formation. This method is more expensive computationally, but offers H_2 performance guarantees and can be applied to cyclic measurement graphs.

4. Time-varying measurement topology

This section and the next extend the analysis of the distributed state observer presented in the previous section to the case where the measurement topology of the formation changes over time. The changes considered here consist in the gain or loss of measurements between vehicles, which can be represented by the addition or removal of edges from the measurement graph $\mathcal{G}_M$ of the formation. When faced with these changes, the local observers must adapt to the new topology as, in general, observer gains computed for a given measurement graph may result in unstable error dynamics when applied to a different topology. Due to this, several new problems arise:

(1) When a change is detected in the available measurements, the vehicles have to compute the new measurement graph.
(2) Once the measurement graph is computed, the vehicles must select suitable local observer gains.
(3) A strategy must be chosen for the local observers to cope with the changes in the formation until the new measurement graph is computed and suitable gains are applied.

4.1. Measurement graph determination

To determine the new measurement topology in a decentralized fashion, the vehicle(s) that lose or gain measurements could execute an algorithm such as the one detailed in Table 1. It is

Table 1
Algorithm for determination of the new measurement graph, for vehicle i.

(1) **Conditions for initialization**: the vehicle gained or lost access to one or more measurements, or received a message generated by step (3) from a neighboring vehicle.

(2) **Initialization**: create a table to store the edges, E_i, and initialize it with the currently known edges, that is, the measurements available to the vehicle. Create a control vector $\mathbf{v}_i \in \mathbb{R}^N$, and set it to zero except for the i-th component, which is set to 1. Create an integer variable *niter* and initialize it to zero, and create a constant *MaxIter* set to the desired maximum number of iterations.

(3) Send E_i and $\mathbf{v}_i$ to neighboring agents (the ones with which communication is available) and wait until the same data is received from them.

(4) Compare E_i with its counterparts received through communication, and add any previously unknown edges. For each nonzero component in each received $\mathbf{v}_j$, set the corresponding component in $\mathbf{v}_i$ to 1.

(5) If all components of $\mathbf{v}_i$ are equal to 1, and if no changes were made to $\mathbf{v}_i$ and E_i in this iteration, stop the algorithm. Increase *niter* by 1. If *niter* $\geq$ *MaxIter*, stop the algorithm. Otherwise, go to (3).

straightforward to verify that, if the communication graph $\mathcal{G}_C$ of the formation is connected, then the algorithm will complete its execution in at most $d_G + 1$ iterations, where d_G is the maximum graph distance in $\mathcal{G}_C$. The upper bound *MaxIter* on the number of iterations is included for the cases in which one or more vehicles become disconnected from the rest of the formation. If the algorithm reaches *MaxIter* iterations, it will stop its execution and the vehicles whose corresponding entry in $\mathbf{v}_i$ is still zero should be considered disconnected from the rest of the formation.

4.2. Selection of new observer gains

After the measurement graph is determined, the vehicles must select and apply suitable observer gains. As the gains for a given topology can be computed beforehand using the methods detailed in Section 3.1, one way to do this would be to store a database of observer gains for a large number of possible measurement graphs on-board each vehicle. Since the local observer gains are constant matrices of relatively low dimension, nowadays it is perfectly feasible to store hundreds or even thousands of precomputed observer gains in each vehicle. However, as the number of possible measurement graphs increases exponentially with the number of vehicles in the formation, it might not be feasible to store gains for all different possible configurations in large formations. However, note that even if gains for a given measurement graph are not available, gains computed for a subgraph of the measurement graph (with the same number of nodes, but fewer edges) are valid: for each measurement also present in the subgraph, apply the corresponding gains and, for the measurements that are missing in the subgraph, set the corresponding observer gains to zero. In this way, the stable error dynamics associated with the subgraph are replicated exactly.

Suppose that each vehicle stores a database of precomputed observer gains for a number of different formation topologies. Following the steps in Table 2 ensures that stabilizing gains for the new formation topology are applied to the local state observers. Note that, in case the first step fails, it is important that all the vehicles choose the same subgraph of the measurement graph, as failing to do so can lead to instability of the estimation error dynamics. It is easy to ensure that this happens by having all vehicles use the same criterion for selecting the subgraph.

4.3. Behavior during transition periods

Regarding the strategy followed by each agent when there are changes in the measurement graph, one possible approach, which is the one used in the simulations in Section 6, is as follows.

- **The vehicle lost measurements**: propagate the dynamics in open loop, that is, set the local observer gains to zero until new gains are selected and applied.
- **The vehicle kept the same measurements, or gained new ones**: keep the old observer gains until new gains are selected and applied.

With this strategy, the transition periods when new measurements appear in the formation are stable, limiting the potential periods of instability to the cases where one or more vehicles lose measurements.

4.4. Assumptions on the measurement and communication graphs

The methods and algorithms discussed in this section addressed the problem of how to deal with a single change in the measurement graph $\mathcal{G}_M$. However, supposing that the measurement and communication graphs $\mathcal{G}_M$ and $\mathcal{G}_C$ may switch multiple times during the mission, they must verify additional assumptions to ensure that the proposed distributed estimation solution functions correctly over time.

Assumption 2. For the discussion on stability in the next section, it is assumed that the following is always verified.

(1) The measurement graph always switches to a stabilizable configuration, that is, for each new measurement graph $\mathcal{G}_M$ there exists a $\mathbf{L}$ which satisfies the structural constraint (6) such that the matrix $(\mathbf{A}_g - \mathbf{L}\mathbf{C}_g)$ of closed-loop estimation error dynamics is Hurwitz stable.
(2) The communication graph $\mathcal{G}_C$ is always connected.
(3) The switches in the measurement graph $\mathcal{G}_M$ are not faster than the determination of said graph. That is, the execution time of the algorithm in Table 1 is bounded by a constant t_G and $t_{i+1} - t_i \geq t_G$, in which $t_1, t_2, t_3, \ldots$ denote the switching times of the measurement graph $\mathcal{G}_M$.

5. Stability analysis

This section details the stability analysis of the error dynamics of the distributed state observer when there are changes in the measurement graph of the formation over time. To model the successive stable operation phases with potentially unstable transition periods between them, switched systems concepts are employed. See Liberzon (2003) for an introduction on switched systems, and Lin and Antsaklis (2009) for a more recent survey on the subject. Results also exist for cases where the systems can switch to unstable configurations, such as in Hespanha, Yakimenko, Kaminer, and Pascoal (2004) and Zhai, Hu, Yasuda, and Michel (2000). The results detailed in this section differ from the ones cited above by being based on the sequential aspect of the switching in the scenario considered in this paper.

If the distributed state observer operates according to what was discussed in the previous section and the graphs associated with the formation verify Assumption 2, its error dynamics can be represented in the following manner: starting at time instant t_0, the error dynamics follow

$$\dot{\tilde{\mathbf{x}}}(t) = (\mathbf{A}_g - \mathbf{L}^1\mathbf{C}_g^1)\tilde{\mathbf{x}}(t) := \mathbf{\Lambda}_1\tilde{\mathbf{x}}(t),$$

with $\mathbf{\Lambda}_1$ Hurwitz. Now, suppose that at $t = t_1$ there is a change in the measurement graph of the formation and assume that, af-

Table 2
Selection of new observer gains.

(1) Search the database for gains corresponding to the new measurement graph. If such gains are found, apply them to the local observer. Otherwise, proceed to step 2.
(2) Search the database for gains corresponding to a subgraph of the new measurement graph. If such gains are found, apply them to the local observer. In this case, the gains corresponding to missing edges are set to zero to preserve stability. If no such gains are found, proceed to step 3.
(3) Remove edges from the new measurement graph to find a directed acyclic subgraph, allowing to apply observer gains independently of the measurement topology at the cost of losing performance (but not stability) guarantees. This process is detailed in Theorem 1 and Remark 3 from Viegas et al. (2012).

ter some time interval no longer than a positive scalar constant τ_u, the vehicles are able to determine the new measurement graph and synchronously apply suitable observer gains. During that time, the error dynamics of the distributed state observer will follow $\dot{\tilde{\mathbf{x}}}(t) = \mathbf{\Lambda}_2\tilde{\mathbf{x}}(t)$, where $\mathbf{\Lambda}_2$ depends on the strategy adopted by the vehicles when losing or gaining measurements, and is possibly unstable. Then, at $t = t_2$, the new observer gains are applied, and the distributed state observer has stable error dynamics

$$\dot{\tilde{\mathbf{x}}}(t) = (\mathbf{A}_g - \mathbf{L}^3\mathbf{C}_g^3)\tilde{\mathbf{x}}(t) := \mathbf{\Lambda}_3\tilde{\mathbf{x}}(t).$$

Now, suppose that these changes in measurement topology continue to happen over time, and the error dynamics alternate sequentially between periods of stability and potential instability. This scenario can be represented by the linear switched system

$$\dot{\boldsymbol{x}}(t) = \mathbf{A}_{\sigma(t)}\boldsymbol{x}(t), \tag{8}$$

where $\boldsymbol{x}(t) \in \mathbb{R}^n$ is the state, $\sigma(t) : [t_0, \infty[\to \mathbb{N}_P = \{1, 2, \ldots, P\}$ is a piecewise constant switching signal, and $\mathbf{A}_\sigma$ takes values in a family of $n \times n$ matrices, $\mathcal{A} := \{\mathbf{A}_p : p \in \mathbb{N}_P\}$. With no loss of generality, assume that $\mathbf{A}_p$ is stable for $1 \le p \le q$, and unstable or marginally stable for $q < p \le P$. Then, there exist scalar constants $a_1 > 0, a_2 > 0, \ldots, a_P > 0, \lambda_1 > 0, \lambda_2 > 0, \ldots, \lambda_q > 0$, and $\lambda_{q+1} \ge 0, \lambda_{q+2} \ge 0, \ldots, \lambda_P \ge 0$ such that

$$\begin{cases} \|e^{\mathbf{A}_p t}\| \le e^{a_p - \lambda_p t}, & 1 \le p \le q \\ \|e^{\mathbf{A}_p t}\| \le e^{a_p + \lambda_p t}, & q < p \le P. \end{cases} \tag{9}$$

Denote the switching times by $t_1, t_2, t_3, \ldots$. Then, to reflect the dynamics of the problem at hand, the switching signal satisfies the following assumption:

Assumption 3. For $t_{2j-2} \le t < t_{2j-1}$, $j \in \mathbb{N}$, the switching signal follows $1 \le \sigma(t) \le q$. For $t_{2j-1} \le t < t_{2j}$, $j \in \mathbb{N}$, the switching signal follows $q < \sigma(t) \le P$. Furthermore, there exists a scalar constant $\tau_u > 0$ such that $(t_{2j} - t_{2j-1}) \le \tau_u$ for all $j \in \mathbb{N}$.

The first part of the assumption encodes the sequential switching between the periods with stable estimation error dynamics and the transition periods in which the error dynamics might be unstable. The second part sets an upper bound τ_u on the duration of the transition periods. It is assumed that, under normal operating conditions, there is a known upper bound on the time the vehicles take to determine the new measurement topology and apply suitable gains, as otherwise it would be impossible to derive stability results.

5.1. Stability of the switched system

Concerning the duration of the stable periods, two different cases are considered. In the first one, the minimum activation time of the stable subsystems is bounded below by a constant:

Assumption 4. There exists a scalar constant $\tau_s > 0$ such that $(t_{2j-1} - t_{2j-2}) \ge \tau_s$ for all $j \in \mathbb{N}$.

As it might not be possible to guarantee a minimum duration on the stable periods, the second case adapts the concept of average dwell time introduced in Hespanha and Morse (1999) to the scenario considered in this paper:

Assumption 5. Let $N_\sigma^u(t_0, t)$ denote the number of switchings to unstable subsystems in the interval $]t_0, t]$. Then, there exists scalar constants $N_0 > 0$ and $\tau_a > 0$ such that, for all $t \ge t_0$,

$$N_\sigma^u(t_0, t) \le N_0 + \frac{t - t_0}{\tau_a}. \tag{10}$$

This assumption states that, on average, the time interval between two consecutive switchings to unstable configurations will be no less than τ_a, and the chatter bound N_0 is included to account for an eventual limited number of faster switchings. If Assumption 3 is also verified, it follows that the duration of each successive "stable/unstable" pair will be, on average, no less than τ_a.

The following result presents a sufficient condition for the stability of (8) for the first case.

Theorem 1. *Consider the linear switched system (8), assume that the switching signal $\sigma(t)$ verifies Assumptions 3 and 4, and let*

$$\alpha^* := \sup_{\substack{1 \le k \le q \\ q < l \le P}} \{a_k - \lambda_k\tau_s + a_l + \lambda_l\tau_u\}.$$

If $\alpha^* < 0$, then there exists a scalar constant $a > 0$ such that the state $\boldsymbol{x}(t)$ of (8) follows

$$\|\boldsymbol{x}(t)\| \le e^{a - \lambda(t - t_0)}\|\boldsymbol{x}(t_0)\|$$

for all $t \ge t_0$ and any $0 < \lambda \le \lambda^*$, with $\lambda^* := -\frac{\alpha^*}{\tau_s + \tau_u}$.

Proof. Let $v \in \mathbb{N}_P$, $w \in \mathbb{N}_P$, $t_v \in \mathbb{R}$, and $t_w \in \mathbb{R}$, and note that

$$\begin{aligned} &a_w + \lambda_w t_w + a_v - \lambda_v t_v \\ &\quad = a_v - \lambda_v\tau_s + a_w + \lambda_w\tau_u - \lambda_v(t_v - \tau_s) + \lambda_w(t_w - \tau_u). \end{aligned} \tag{11}$$

Assume that $1 \le v \le q$, $q < w \le P$, $t_v \ge \tau_s$, and $t_w \le \tau_u$. Then, it can be shown that, for any $0 < \lambda \le \lambda^*$, the following inequalities are verified:

$$\begin{cases} a_v - \lambda_v\tau_s + a_w + \lambda_w\tau_u \le -\lambda(\tau_s + \tau_u) \\ -\lambda_v(t_v - \tau_s) \le -\lambda^*(t_v - \tau_s) \le -\lambda(t_v - \tau_s) \\ \lambda_w(t_w - \tau_u) \le 0 \le -\lambda(t_w - \tau_u). \end{cases} \tag{12}$$

Then, taking the exponential of (11) and using (12) yields

$$e^{a_w + \lambda_w t_w + a_v - \lambda_v t_v} \le e^{-\lambda(t_w + t_v)}. \tag{13}$$

Let p_l denote the value of $\sigma(t)$ between t_l and t_{l+1}. Then, for any $j > 0$ and any t such that $t_j \le t \le t_{j+1}$, the state of the system (8) follows

$$\boldsymbol{x}(t) = e^{\mathbf{A}_{p_j}(t - t_j)}e^{\mathbf{A}_{p_{j-1}}(t_j - t_{j-1})} \ldots e^{\mathbf{A}_{p_0}(t_1 - t_0)}\boldsymbol{x}(t_0),$$

and its norm verifies the inequality

$$\|\boldsymbol{x}(t)\| \le \|e^{\mathbf{A}_{p_j}(t - t_j)}\| \prod_{l=1}^{j} \left(\|e^{\mathbf{A}_{p_{l-1}}(t_l - t_{l-1})}\|\right) \|\boldsymbol{x}(t_0)\|. \tag{14}$$

Suppose that at time t the system (8) is in an unstable configuration, and let $j^* = \lfloor j/2 \rfloor$. Using (9) in (14) yields

$$\|\boldsymbol{x}(t)\| \le \|\boldsymbol{x}(t_0)\| e^{a_{p_j} + \lambda_{p_j}(t - t_j) + a_{p_{j-1}} - \lambda_{p_{j-1}}(t_j - t_{j-1})}$$
$$\prod_{l=1}^{j^*} \left(e^{a_{p_{2l-1}} + \lambda_{p_{2l-1}}(t_{2l} - t_{2l-1}) + a_{p_{2l-2}} - \lambda_{p_{2l-2}}(t_{2l-1} - t_{2l-2})}\right),$$

and applying the inequality (13) results in

$$\begin{aligned}\|\boldsymbol{x}(t)\| &\leq e^{-\lambda(t-t_{j-1})}\prod_{l=1}^{j^*}\left(e^{-\lambda(t_{2l}-t_{2l-2})}\right)\|\boldsymbol{x}(t_0)\|\\ &\leq e^{-\lambda(t-t_0)}\|\boldsymbol{x}(t_0)\|.\end{aligned}$$

On the other hand, if at time t the system (8) is in a stable configuration, following the same reasoning yields

$$\begin{aligned}\|\boldsymbol{x}(t)\| &\leq e^{a_j-\lambda(t-t_j)}\prod_{l=1}^{j*}\left(e^{-\lambda(t_{2l}-t_{2l-2})}\right)\|\boldsymbol{x}(t_0)\|\\ &\leq e^{a_j-\lambda(t-t_0)}\|\boldsymbol{x}(t_0)\|. \quad \square\end{aligned}$$

The following result presents a sufficient condition for the stability of (8) for the second case.

Theorem 2. *Consider the switched linear system (8), assume that the switching signal $\sigma(t)$ verifies Assumptions 3 and 5, and let*

$$\alpha_a^* := a_s + a_u + \lambda_s\tau_u + \lambda_u\tau_u - \lambda_s\tau_a,$$

where

$$a_s = \sup_{1\leq k\leq q}\{a_k\}, \qquad a_u = \sup_{q<k\leq P}\{a_k\},$$
$$\lambda_s = \inf_{1\leq k\leq q}\{\lambda_k\}, \quad \text{and} \quad \lambda_u = \sup_{q<k\leq P}\{\lambda_k\}.$$

Then, if $\alpha_a^* < 0$, there exists a scalar constant $a > 0$ such that the state $\boldsymbol{x}(t)$ of (8) follows

$$\|\boldsymbol{x}(t)\| \leq e^{a-\lambda(t-t_0)}\|\boldsymbol{x}(t_0)\|$$

for all $t \geq t_0$ and any $0 < \lambda \leq \lambda_a^*$, where $\lambda_a^* := -\frac{\alpha_a^*}{\tau_a}$.

Proof. As in the previous case, for any $j > 0$ and any t such that $t_j \leq t \leq t_{j+1}$, the norm of the state of the system (8) verifies

$$\|\boldsymbol{x}(t)\| \leq \|e^{\mathbf{A}_{p_j}(t-t_j)}\|\prod_{l=1}^{j}\left(\|e^{\mathbf{A}_{p_{l-1}}(t_l-t_{l-1})}\|\right)\|\boldsymbol{x}(t_0)\|. \tag{15}$$

Now, denote the total activation time of stable subsystems on $[t_0, t]$ by $T_s(t_0, t)$, the total activation time of unstable systems on $[t_0, t]$ by $T_u(t_0, t)$, and the number of switchings to stable subsystems on $]t_0, t]$ by $N_\sigma^s(t_0, t)$. Then, using (9) in (15), it follows that

$$\|\boldsymbol{x}(t)\| \leq e^{(N_\sigma^s(t_0,t)+1)a_s+N_\sigma^u(t_0,t)a_u}e^{-\lambda_s T_s(t_0,t)+\lambda_u T_u(t_0,t)}\|\boldsymbol{x}(t_0)\|. \tag{16}$$

Due to Assumption 3, $N_\sigma^s(t_0, t) \leq N_\sigma^u(t_0, t)$, and (16) can be rewritten as

$$\|\boldsymbol{x}(t)\| \leq e^{a_s+N_\sigma^u(t_0,t)(a_s+a_u)-\lambda_s T_s(t_0,t)+\lambda_u T_u(t_0,t)}\|\boldsymbol{x}(t_0)\|. \tag{17}$$

As

$$T_u(t_0, t) \leq N_\sigma^u(t_0, t)\tau_u, \tag{18}$$

it follows that

$$T_s(t_0, t) = (t - t_0) - T_u(t_0, t) \geq (t - t_0) - N_\sigma^u(t_0, t)\tau_u. \tag{19}$$

Using (18) and (19) in (17) yields

$$\|\boldsymbol{x}(t)\| \leq e^{a_s+N_\sigma^u(t_0,t)(a_s+a_u+\lambda_s\tau_u+\lambda_u\tau_u)-\lambda_s(t-t_0)}\|\boldsymbol{x}(t_0)\|$$

and, given (10), it follows that

$$\|\boldsymbol{x}(t)\| \leq e^{a-\frac{\alpha_a^*}{\tau_a}(t-t_0)}\|\boldsymbol{x}(t_0)\|,$$

with $a = a_s + N_0(a_s + a_u + \lambda_s\tau_u + \lambda_u\tau_u)$. Then, for any $0 < \lambda \leq \lambda_a^*$, the inequality $\|\boldsymbol{x}(t)\| \leq e^{a-\lambda(t-t_0)}\|\boldsymbol{x}(t_0)\|$ is verified for all $t \geq t_0$, which concludes the proof. $\square$

6. Simulations for a formation of AUVs

This section details the application of the results introduced in the previous sections to the practical case of decentralized position and velocity estimation in a formation of AUVs, supported by simulation results.

Consider a formation composed of N AUVs, and suppose that each has sensors mounted on-board which give access to either measurements of its own position in an inertial reference coordinate frame $\{I\}$, or measurements of its position relative to one or more AUVs in the vicinity, as well as updated position estimates communicated by those same AUVs. For the first case, i.e., with inertial position readings, the local dynamics for AUV i follow

$$\begin{cases}\dot{\mathbf{p}}_i(t) = \mathbf{R}_i(t)\mathbf{v}_i(t)\\ \dot{\mathbf{v}}_i(t) = -\mathbf{S}(\boldsymbol{\omega}_i(t))\mathbf{v}_i(t) + \mathbf{g}_i(t) + \mathbf{a}_i(t)\\ \dot{\mathbf{g}}_i(t) = -\mathbf{S}(\boldsymbol{\omega}_i(t))\mathbf{g}_i(t)\\ \mathbf{y}_i(t) = \mathbf{p}_i(t),\end{cases}$$

where $\mathbf{p}_i(t) \in \mathbb{R}^3$ is the inertial position of the vehicle, $\mathbf{v}_i(t) \in \mathbb{R}^3$ denotes its velocity relative to $\{I\}$, expressed in body-fixed coordinates of the i-th AUV, $\mathbf{R}_i(t) \in SO(3)$ is the rotation matrix from the body-fixed frame $\{B_i\}$ of the vehicle to $\{I\}$, $\boldsymbol{\omega}_i(t) \in \mathbb{R}^3$ is the angular velocity of $\{B_i\}$, expressed in body-fixed coordinates, $\mathbf{S}(\boldsymbol{\omega})$ is the skew-symmetric matrix such that $\mathbf{S}(\boldsymbol{\omega})\boldsymbol{x}$ is the cross product $\boldsymbol{\omega} \times \boldsymbol{x}$, $\mathbf{a}_i(t) \in \mathbb{R}^3$ is a linear acceleration measurement provided by an accelerometer mounted on-board each AUV, and $\mathbf{g}_i(t) \in \mathbb{R}^3$ is the acceleration of gravity expressed in body-fixed coordinates, which is treated as an unknown variable for performance reasons, see Batista, Silvestre, and Oliveira (2010) for further details. It is assumed that an Attitude and Heading Reference System (AHRS) installed on-board each AUV provides measurements of both $\mathbf{R}_i(t)$ and $\boldsymbol{\omega}_i(t)$.

Using the state transformation introduced in Batista, Silvestre, and Oliveira (2009),

$$\begin{bmatrix}\mathbf{x}_i^1(t)\\ \mathbf{x}_i^2(t)\\ \mathbf{x}_i^3(t)\end{bmatrix} := \begin{bmatrix}\mathbf{I} & \mathbf{0} & \mathbf{0}\\ \mathbf{0} & \mathbf{R}_i(t) & \mathbf{0}\\ \mathbf{0} & \mathbf{0} & \mathbf{R}_i(t)\end{bmatrix}\begin{bmatrix}\mathbf{p}_i(t)\\ \mathbf{v}_i(t)\\ \mathbf{g}_i(t)\end{bmatrix}, \tag{20}$$

which preserves stability and observability properties (Brockett, 1970), and making $\mathbf{u}_i(t) := \mathbf{R}_i(t)\mathbf{a}_i(t)$, the system dynamics can be written as the LTI system (1), with

$$\mathbf{A}_L = \begin{bmatrix}\mathbf{0} & \mathbf{I} & \mathbf{0}\\ \mathbf{0} & \mathbf{0} & \mathbf{I}\\ \mathbf{0} & \mathbf{0} & \mathbf{0}\end{bmatrix}, \qquad \mathbf{B}_L = \begin{bmatrix}\mathbf{0}\\ \mathbf{I}\\ \mathbf{0}\end{bmatrix}, \quad \text{and} \quad \mathbf{C}_L = \begin{bmatrix}\mathbf{I} & \mathbf{0} & \mathbf{0}\end{bmatrix}.$$

When the AUV has access to relative position measurements and receives position estimates from the corresponding vehicles, the local dynamics for AUV i follow

$$\begin{cases}\dot{\mathbf{p}}_i(t) = \mathbf{R}_i(t)\mathbf{v}_i(t)\\ \dot{\mathbf{v}}_i(t) = -\mathbf{S}(\boldsymbol{\omega}_i(t))\mathbf{v}_i(t) + \mathbf{g}_i(t) + \mathbf{a}_i(t)\\ \dot{\mathbf{g}}_i(t) = -\mathbf{S}(\boldsymbol{\omega}_i(t))\mathbf{g}_i(t)\\ \mathbf{y}_i(t) = \Delta\mathbf{p}_i(t),\end{cases}$$

in which $\Delta\mathbf{p}_i(t)$ denotes the relative position measurements available to AUV i. Applying (20) yields the system (2), where $\mathbf{A}_L$ and $\mathbf{B}_L$ are defined as in the previous case, and $\mathbf{C}_i = \mathbf{I}_{N_i} \otimes \mathbf{C}_L \in \mathbb{R}^{o_L N_i \times n_L N_i}$. Following this, a local state estimator can be designed for each AUV resulting in a distributed state observer with estimation error dynamics given by (7). The local observers are then implemented in the body-fixed coordinate space of each AUV, by reversing the Lyapunov state transformation (20). This process is described in detail in Viegas et al. (2012).

To assess the stability of the proposed solution, simulations were carried out for a formation of 6 AUVs, whose structure alternates between the 4 measurement graphs depicted in Fig. 2.

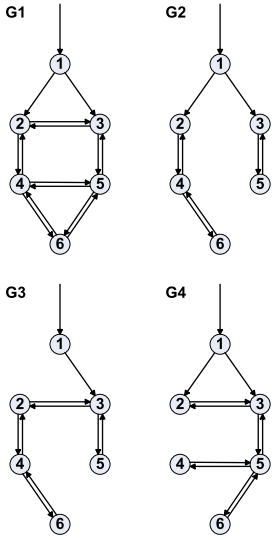

Fig. 2. Formation graphs considered in the simulations.

Table 3
Bounding constants for each measurement graph and the worst case of the transition periods.

Graph	G1	G2	G3	G4	Transition
a	2.655	2.297	2.861	2.964	3.861
λ	−0.118	−0.089	−0.092	−0.104	0.1

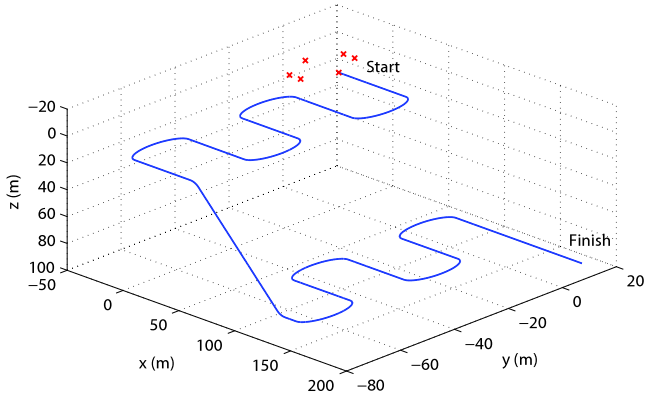

Fig. 3. Initial positions and trajectory followed by the AUVs.

In line with the stability analysis of Section 5, Table 3 details bounding constants that were computed for the error dynamics of the distributed state observer for each measurement graph, as well as for the worst case of the transition periods. Using the values in Table 3 and the results of Section 4.3, it can be concluded, for example, that if the unstable transition times last at most $\tau_u = 10$ s, then stability is guaranteed if the stable periods last at least $\tau_s = 85$ s, approximately. However, those figures are conservative, as it will be seen in the simulation results that follow.

The durations of the stable configurations were computed by sampling a normal distribution with an expected value of $t_s = 75$ s and a standard deviation of $\sigma_s = 15$ s, while the duration of the transition periods follows a normal distribution with an expected value of $t_u = 15$ s and a standard deviation of $\sigma_u = 1$ s. The measurement graph and observer gains changed following a randomly generated sequence. The initial positions of the AUVs, as well as the trajectory followed by the formation, are depicted in Fig. 3. Fig. 4 depicts the evolution and a detailed view of the sum of the modulus of all estimation error variables in the formation. As it can be seen, during the unstable periods the estimation error

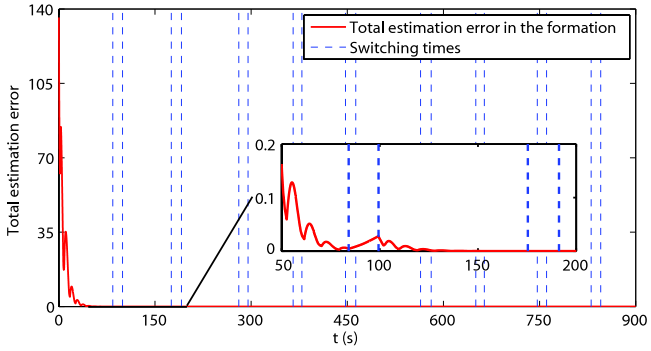

Fig. 4. Total estimation error in the formation.

increases, but the stable periods last long enough to stabilize the error dynamics.

7. Conclusions

This paper addressed the problem of distributed state estimation in formations of vehicles with time-varying measurement topology. The proposed solution consists in the implementation of a local state observer on-board each vehicle, resulting in a distributed state estimator at the formation level. A strategy was outlined for the vehicles to cope with the gain or loss of measurements and to apply new gains that stabilize the new error dynamics. The error dynamics of the distributed state estimator were modeled as a switched linear system, and sufficient conditions for exponential stability of the global estimation error dynamics were presented for two different switching laws. The results were then applied to the practical case of a formation of Autonomous Underwater Vehicles (AUVs), and simulations were detailed to verify the stability of the proposed decentralized state estimator.

Acknowledgments

This work was supported by the Fundação para a Ciência e a Tecnologia (FCT) through ISR under LARSyS PEst-OE/EEI/LA0009, and through IDMEC, under LAETA UID/EMS/50022/2013 projects and by the FCT project PTDC/EEACRO/111197/2009 MAST/AM. The work of D. Viegas was supported by the Ph.D. Student Scholarship SFRH/BD/71486/2010, from FCT.

References

Astrom, K. J., & Murray, R. M. (2008). *Feedback systems: an introduction for scientists and engineers*. Princeton University Press.
Barooah, Prabir (2007). *Estimation and control with relative measurements: algorithms and scaling laws*. (Ph.D. thesis), Santa Barbara: University of California, September.
Batista, P., Silvestre, C., & Oliveira, P. (2009). Position and velocity optimal sensor-based navigation filters for UAVs. In *Proceedings of the 2009 American control conference, Saint Louis, USA, June* (pp. 5404–5409).
Batista, P., Silvestre, C., & Oliveira, P. (2010). Optimal position and velocity navigation filters for autonomous vehicles. *Automatica*, *46*(4), 767–774.
Bender, J. G. (1991). An overview of systems studies of automated highway systems. *IEEE Transactions on Vehicular Technology*, *40*(1), 82–99.
Brockett, R. W. (1970). *Finite dimensional linear systems*. Wiley and Sons.
Chen, C. L. P., Wen, Guo-Xing, Liu, Yan-Jun, & Wang, Fei-Yue (2014). Adaptive consensus control for a class of nonlinear multiagent time-delay systems using neural networks. *IEEE Transactions on Neural Networks and Learning Systems*, *25*(6), 1217–1226.
Curtin, T., Bellingham, J., & Webb, D. (1993). Autonomous oceanographic sampling networks. *Oceanography*, *6*, 86–94.
Fax, J. Alexander (2002). *Optimal and cooperative control of vehicle formations*. (Ph.D. thesis), California Institute of Technology.
Giulietti, F., Pollini, L., & Innocenti, M. (2000). Autonomous formation flight. *IEEE Control Systems Magazine*, *20*(6), 34–44.
Hespanha, J. P., & Morse, A. S. (1999). Stability of switched systems with average dwell-time. In *Proceedings of the 38th IEEE conference on decision and control, Vol. 3, Phoenix, Arizona, USA, December* (pp. 2655–2660).
Hespanha, J., Yakimenko, O., Kaminer, I., & Pascoal, A. (2004). Linear parametrically varying systems with brief instabilities: application to vision/inertial navigation. *IEEE Transactions on Aerospace and Electronic Systems*, *40*(3), 889–902.

Lessard, L., & Lall, S. (2011). Quadratic invariance is necessary and sufficient for convexity. In *Proceedings of the 2011 American control conference, San Francisco, CA, USA, July* (pp. 5360–5362).
Liberzon, D. (2003). *Switching in systems and control*. Birkhäuser.
Lin, H., & Antsaklis, P. (2009). Stability and stabilizability of switched linear systems: a survey of recent results. *IEEE Transactions on Automatic Control, 54*(2), 308–322.
Rokowitz, M. (2008). On information structures, convexity, and linear optimality. In *Proceedings of the 47th IEEE conference on decision and control, Cancun, Mexico, December* (pp. 1642–1647).
Sousa, R., Oliveira, P., & Gaspar, T. (2009). Joint positioning and navigation aiding systems for multiple underwater robots. In *8th IFAC conference on manoeuvring and control of marine craft, Guaruja, Brazil, September* (pp. 167–172).
Tanner, H. G., & Christodoulakis, D. K. (2007). Decentralized cooperative control of heterogeneous vehicle groups. *Robotics and Autonomous Systems*, *55*(11).
Viegas, D., Batista, P., Oliveira, P., & Silvestre, C. (2012). Decentralized H_2 observers for position and velocity estimation in vehicle formations with fixed topologies. *Systems & Control Letters*, *61*(3), 443–453.
Viegas, D., Batista, P., Oliveira, P., & Silvestre, C. (2013). Decentralized linear state observers for vehicle formations with time-varying topologies. In *2013 American control conference, Washington, DC, USA, June*.
Yuan, Y., & Tanner, H. G. (2010). Sensor graphs for guaranteed cooperative localization performance. *Control and Intelligent Systems*, *38*(1), 32–39.
Zhai, G., Hu, B., Yasuda, K., & Michel, A. N. (2000). Stability analysis of switched systems with stable and unstable subsystems: an average dwell-time approach. In *Proceedings of the 2000 American control conference, Chicago, Illinois, USA, June* (pp. 200–204).

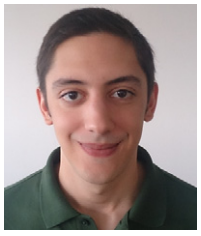

Daniel Viegas received the M.Sc. degree in Electrical and Computer Engineering in 2010 from Instituto Superior Técnico (IST), Lisbon, Portugal. He is currently a Ph.D. student at the Institute for Systems and Robotics (ISR) at IST. His research interests include distributed state estimation, observers for nonlinear systems, and Kalman filtering.

Pedro Batista (M'10) received the Licenciatura degree in Electrical and Computer Engineering in 2005 and the Ph.D. degree in 2010, both from Instituto Superior Técnico (IST), Lisbon, Portugal. From 2004 to 2006, he was a Monitor with the Department of Mathematics, IST, where he is currently an Invited Assistant Professor with the Department of Electrical and Computer Engineering. His research interests include sensor-based navigation and control of autonomous vehicles. Dr. Batista has received the Diploma de Mérito twice during his graduation and his Ph.D. thesis was awarded the Best Robotics Ph.D. Thesis Award by the Portuguese Society of Robotics.

Paulo Oliveira received the Ph.D. degree in Electrical and Computer Engineering, from the Instituto Superior Técnico (IST), Lisbon, Portugal, in 2002. He is Associate Professor in the Department of Mechanical Engineering of IST and researcher in the Institute of Mechanical Engineering, IST. He also collaborates with the Institute for Systems and Robotics, IST. His areas of scientific activity are Mechatronics with special focus on the fields of Autonomous Vehicles, Robotics, Sensor Fusion, Navigation, Positioning, and Nonlinear Estimation. Over the last 25 years he participated in more than 30 European and Portuguese research projects and he co-authored more than 50 journal and 150 conference papers.

Carlos Silvestre received the Licenciatura degree in Electrical Engineering from the Instituto Superior Técnico (IST) of Lisbon, Portugal, in 1987 and the M.Sc. degree in Electrical Engineering and the Ph.D. degree in Control Science from the same school in 1991 and 2000, respectively. In 2011 he received the Habilitation in Electrical Engineering and Computers also from IST. Since 2000, he is with the Department of Electrical Engineering of the Instituto Superior Técnico, where he is currently an Associate Professor of Control and Robotics on leave. Since 2012 he is an Associate Professor of the Department of Electrical and Computers Engineering of the Faculty of Science and Technology of the University of Macau. Over the past years, he has conducted research on the subjects of navigation guidance and control of air and underwater robots. His research interests include linear and nonlinear control theory, coordinated control of multiple vehicles, gain scheduled control, integrated design of guidance and control systems, inertial navigation systems, and mission control and real time architectures for complex autonomous systems with applications to unmanned air and underwater vehicles.

C. L. Philip Chen (S'88–M'88–SM'94–F'07) received the M.S. degree in electrical engineering from the University of Michigan, Ann Arbor, in 1985 and the Ph.D. degree in electrical engineering from Purdue University, West Lafayette, IN, in 1988. After having worked at US for 23 years as a tenured professor, as a department head and associate dean in two different universities, he is currently the Dean of the Faculty of Science and Technology, University of Macau, Macau, China and a Chair Professor of the Department of Computer and Information Science. Dr. Chen is a Fellow of the IEEE and the AAAS. Currently, he is the Editor-in-Chief of IEEE Transactions on Systems, Man, and Cybernetics: Systems (2014–) and associate editors of several IEEE Transactions. He is also the Chair of TC 9.1 Economic and Business Systems of IFAC. His research areas are systems, cybernetics, and computational intelligence.